New Zwitterionic Spirocyclic λ^5*Si*-Silicates with an *Si*X_4C Skeleton (X = S, O) Containing Two Ligands of the Dithiolato(2−) or Diolato(2−) Type: Synthesis, Structure, and Bonding Situation§

Rüdiger Bertermann, Andreas Biller, Martin Kaupp, Martin Penka, Oliver Seiler, and Reinhold Tacke*

Institut für Anorganische Chemie, Universität Würzburg, Am Hubland, D-97074 Würzburg, Germany

Received April 23, 2003

Reaction of trimethoxy(morpholinomethyl)silane (**7**) with lithium aluminum hydride yielded (morpholinomethyl)silane (**8**). Treatment of **8** with ethane-1,2-dithiol (molar ratio 1:2) in MeCN afforded bis[ethane-1,2-dithiolato(2−)](morpholiniomethyl)silicate (**5**; isolated as **5**·MeCN). Reaction of **7** with ethane-1,2-diol (molar ratio 1:2) in MeCN yielded the oxygen analogue bis[ethane-1,2-diolato(2−)](morpholiniomethyl)silicate (**6**). Single-crystal X-ray diffraction studies showed that the Si-coordination polyhedra of **5**·MeCN and **6** are distorted trigonal bipyramids. Compounds **5**·MeCN and **6** were additionally characterized by solid-state VACP/MAS NMR experiments (^{13}C, ^{29}Si). The structural investigations were complemented by quantum-chemical studies of the structure, bonding, and ^{29}Si NMR chemical shift tensors of **5** (*Si*S_4C skeleton) and **6** (*Si*O_4C skeleton).

Introduction

In context with our studies on zwitterionic silicates with pentacoordinate silicon atoms,[1] we have recently reported on the synthesis and structural characterization of zwitterionic silicon(IV) complexes containing two bidentate ligands of the dithiolato(2−) or oatothiolato(2−) type, compounds **1**,[2] **2**,[2] **3**,[3] and **4**[3] (Chart 1). The realization of the hitherto unknown bonding situations at the pentacoordinate silicon atoms of **1**−**4** (*Si*S_4C or *Si*O_2S_2C skeletons) was accomplished by using the "zwitterion trick". Generally, such zwitterionic pentacoordinate silicates (which contain a formally negatively charged silicon atom and a formally positively charged nitrogen atom) are characterized by an excellent crystallizability. This particular property is very advantageous for their preparation and isolation and for their structural characterization by single-crystal X-ray diffraction and solid-state NMR spectroscopy. In addition, most of the zwitterionic pentacoordinate silicates studied so far were found to exist in solution as well and therefore could be studied for their structure and dynamic behavior by solution NMR spectroscopy.

We have now succeeded in synthesizing a further zwitterionic λ^5*Si*-silicate with an *Si*S_4C framework, compound **5**·MeCN, and we have studied the anisotropy

Chart 1

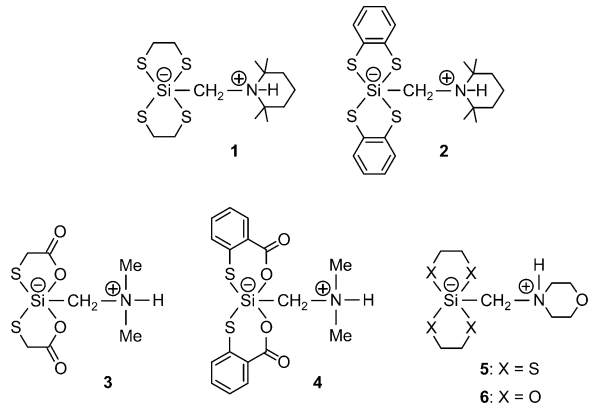

of the ^{29}Si chemical shift (solid-state NMR experiments), which was expected to respond very sensitively to structure and bonding. For reasons of comparison, the oxygen analogue **6** (*Si*O_4C skeleton) was also synthesized and analyzed by solid-state ^{29}Si NMR spectroscopy. We were especially interested in evaluating the potential usefulness of solid-state NMR spectroscopy, combined with quantum-chemical calculations, in the structural characterization of pentacoordinate silicon complexes. This approach could become particularly important in those cases where single-crystal X-ray diffraction studies are not possible.

We report here on the synthesis of compounds **5**·MeCN and **6** and their characterization in the solid state (crystal structure analyses; ^{13}C and ^{29}Si VACP/MAS NMR experiments). To get more information about the nature of the analogous *Si*S_4C and *Si*O_4C frameworks of **5** and **6**, these experimental investigations were complemented by computational studies of the struc-

§ Dedicated to Professor Wolfgang Malisch on the occasion of his 60th birthday.

* To whom correspondence should be addressed. E-mail: r.tacke@mail.uni-wuerzburg.de.

(1) Review dealing with zwitterionic λ^5*Si*-silicates: Tacke, R.; Pülm, M.; Wagner, B. *Adv. Organomet. Chem.* **1999**, *44*, 221−273, and references therein.

(2) Tacke, R.; Mallak, M.; Willeke, R. *Angew. Chem.* **2001**, *113*, 2401−2403; *Angew. Chem. Int. Ed.* **2001**, *40*, 2339−2341.

(3) Willeke, R.; Tacke, R. *Z. Anorg. Allg. Chem.* **2001**, *627*, 1537−1541.

10.1021/om030301s CCC: $25.00
Publication on Web 09/04/2003

ture, bonding, and ^{29}Si NMR chemical shift tensors of **5** and **6**. In particular, we were interested to learn to what extent the ^{29}Si chemical shift tensors are characteristic of the bonding situation at the pentacoordinate silicon atoms of **5** and **6** (for reviews dealing with compounds of higher-coordinate silicon, see refs 1 and 4).

Results and Discussion

Syntheses. Bis[ethane-1,2-dithiolato(2−)](morpholiniomethyl)silicate (**5**) was prepared by a two-step synthesis, starting from trimethoxy(morpholinomethyl)-silane (**7**) (Scheme 1). Treatment of **7** with lithium

Scheme 1

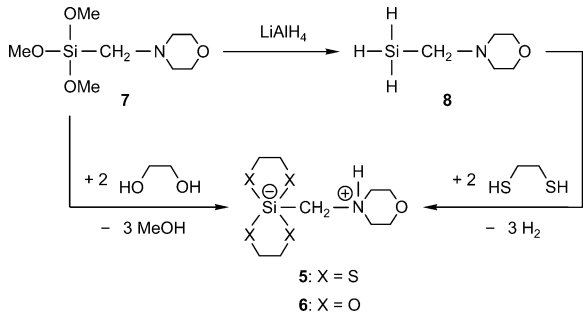

aluminum hydride in diethyl ether afforded (morpholinomethyl)silane (**8**), which was isolated in 61% yield as a colorless liquid. Subsequent reaction of **8** with 2 molar equiv of ethane-1,2-dithiol in acetonitrile gave compound **5**, which was isolated in 86% yield as the colorless crystalline solvate **5**·MeCN. Bis[ethane-1,2-diolato(2−)](morpholiniomethyl)silicate (**6**) was synthesized by reaction of **7** with 2 molar equiv of ethane-1,2-diol in acetonitrile and isolated, after recrystallization from dichloromethane/diethyl ether, in 80% yield as a colorless crystalline solid (Scheme 1). The identities of **5**·MeCN and **6** were established by elemental analyses (C, H, N, S), solid-state ^{13}C and ^{29}Si VACP/MAS NMR studies, and crystal structure analyses.

Crystal Structure Analyses. The crystal data and the experimental parameters used for the crystal structure analyses of **5**·MeCN and **6** are summarized in Table 1; selected interatomic distances and angles are listed in Table 2. The structures of **5** and **6** are depicted in Figures 1 and 2.

The zwitterions **5** and **6** are chiral, and the crystals of **5**·MeCN and **6** contain pairs of the respective Λ- and Δ-enantiomers. As can be seen from Figures 1 and 2 and Table 2, the Si-coordination polyhedra of the title compounds are somewhat distorted trigonal bipyramids, with each bidentate dithiolato(2−) or diolato(2−) ligand

Table 1. Crystal Data and Experimental Parameters for the Crystal Structure Analyses of 5·MeCN and 6

	5·MeCN	**6**
empirical formula	$C_{11}H_{22}N_2OS_4Si$	$C_9H_{19}NO_5Si$
formula mass, g mol^{-1}	354.64	249.34
collection T, K	173(2)	173(2)
λ(Mo Kα), Å	0.71073	0.71073
cryst syst	monoclinic	orthorhombic
space group (No.)	$P2_1/c$ (14)	$Fdd2$ (43)
a, Å	8.1159(16)	14.795(2)
b, Å	10.785(2)	37.143(4)
c, Å	19.094(4)	8.5256(9)
β, deg	98.64(3)	90
V, Å^3	1652.4(6)	4685.1(10)
Z	4	16
D(calcd), g cm^{-3}	1.426	1.414
μ, mm^{-1}	0.641	0.207
F(000)	752	2144
cryst dimens, mm	0.5 × 0.1 × 0.1	0.5 × 0.5 × 0.1
2θ range, deg	4.32−53.92	5.92−53.86
index ranges	$-9 \le h \le 9$	$-18 \le h \le 18$
	$-13 \le k \le 13$	$-47 \le k \le 46$
	$-24 \le l \le 24$	$-10 \le l \le 10$
no. of collected reflns	21928	13853
no. of indep reflns	3347	2486
R_{int}	0.0598	0.0603
no. of reflns used	3347	2486
no. of params	176	148
S^a	1.026	1.070
weight params a/b^b	0.0394/1.3682	0.0551/1.5858
R1^c [$I > 2\sigma(I)$]	0.0326	0.0292
wR2^d (all data)	0.0821	0.0767
max./min. residual electron density, e Å^{-3}	+0.305/−0.315	+0.321/−0.275

^{a} $S = \{\sum[w(F_o^2 - F_c^2)^2]/(n - p)\}^{0.5}$; n = no. of reflections; p = no. of parameters. ^{b} $w^{-1} = \sigma^2(F_o^2) + (aP)^2 + bP$, with $P = [(\max F_o^2,0) + 2F_c^2]/3$. ^{c} $R1 = \sum||F_o| - |F_c||/\sum|F_o|$. ^{d} $wR2 = \{\sum[w(F_o^2 - F_c^2)^2]/\sum[w(F_o^2)^2]\}^{0.5}$.

Table 2. Selected Interatomic Distances (Å) and Angles (deg) for 5 and 6 Obtained by Crystal Structure Analyses of 5·MeCN and 6 (Exptl) and by Geometry Optimizations of 5 and 6 (Calcd)

	5·MeCN^a (exptl)	**6**^{b} (exptl)	**5**^{a} (calcd)	**5**, dimer^a (calcd)	**6**^{b} (calcd)
Si−X1	2.3475(8)	1.7370(10)	2.438	2.408	1.854
Si−X2	2.1728(9)	1.6916(10)	2.190	2.183	1.704
Si−X3	2.2926(8)	1.7700(10)	2.244	2.259	1.743
Si−X4	2.1725(9)	1.6962(10)	2.167	2.183	1.705
Si−C1	1.927(2)	1.9104(13)	1.954	1.940	1.949
X1−Si−X2	90.16(3)	90.24(5)	90.3	90.2	87.7
X1−Si−X3	174.44(3)	176.92(5)	177.5	178.3	178.1
X1−Si−X4	86.76(3)	91.61(5)	84.9	85.2	88.9
X1−Si−C1	96.03(6)	94.85(5)	86.8	92.3	86.7
X2−Si−X3	86.47(3)	86.80(5)	92.0	90.9	93.3
X2−Si−X4	127.27(4)	121.44(5)	123.6	122.9	123.9
X2−Si−C1	118.80(8)	122.22(6)	114.1	118.7	118.7
X3−Si−X4	91.75(3)	89.23(5)	94.4	93.1	91.8
X3−Si−C1	89.48(6)	87.45(5)	91.5	88.4	91.4
X4−Si−C1	113.87(8)	115.90(6)	121.6	118.3	117.0

^{a} X = S. ^{b} X = O.

(4) Selected reviews dealing with higher-coordinate silicon compounds: (a) Tandura, S. N.; Voronkov, M. G.; Alekseev, N. V. *Top. Curr. Chem.* **1986**, *131*, 99−189. (b) Sheldrick, W. S. In *The Chemistry of Organic Silicon Compounds*; Patai, S., Rappoport, Z., Eds.; Wiley: Chichester, U.K., 1989; Part 1, pp 227−303. (c) Bassindale, A. R.; Taylor, P. G. In *The Chemistry of Organic Silicon Compounds*; Patai, S., Rappoport, Z., Eds.; Wiley: Chichester, U.K., 1989; Part 1, pp 839−892. (d) Corriu, R. J. P.; Young, J. C. In *The Chemistry of Organic Silicon Compounds*; Patai, S., Rappoport, Z., Eds.; Wiley: Chichester, U.K., 1989; Part 2, pp 1241−1288. (e) Holmes, R. R. *Chem. Rev.* **1990**, *90*, 17−31. (f) Chuit, C.; Corriu, R. J. P.; Reye, C.; Young, J. C. *Chem. Rev.* **1993**, *93*, 1371−1448. (g) Tacke, R.; Becht, J.; Lopez-Mras, A.; Sperlich, J. *J. Organomet. Chem.* **1993**, *446*, 1−8. (h) Wong, C. Y.; Woollins, J. D. *Coord. Chem. Rev.* **1994**, *130*, 175−241. (i) Verkade, J. G. *Coord. Chem. Rev.* **1994**, *137*, 233−295. (j) Tacke, R.; Dannappel, O. In *Tailor-made Silicon-Oxygen Compounds−From Molecules to Materials*; Corriu, R., Jutzi, P., Eds.; Vieweg: Braunschweig, Wiesbaden, Germany, 1996; pp 75−86. (k) Lukevics, E.; Pudova, O. A. *Chem. Heterocycl. Compd. (Engl. Transl.)* **1996**, *32*, 1381−1418. (l) Holmes, R. R. *Chem. Rev.* **1996**, *96*, 927−950. (m) Kost, D.; Kalikhman, I. In *The Chemistry of Organic Silicon Compounds*; Rappoport, Z., Apeloig, Y., Eds.; Wiley: Chichester, U.K., 1998; Vol. 2, Part 2, pp 1339−1445. (n) Pestunovich, V.; Kirpichenko, S.; Voronkov, M. In *The Chemistry of Organic Silicon Compounds*; Rappoport, Z., Apeloig, Y., Eds.; Wiley: Chichester, U.K., 1998; Vol. 2, Part 2, pp 1447−1537. (o) Chuit, C.; Corriu, R. J. P.; Reye, C. In *Chemistry of Hypervalent Compounds*; Akiba, K., Ed.; Wiley-VCH: New York, 1999; pp 81−146. (p) Brook, M. A. *Silicon in Organic, Organometallic, and Polymer Chemistry*; Wiley: New York, 2000; pp 97−114.

Table 3. Hydrogen-Bonding Geometries for 5·MeCN and 6[a]

	D−H···A	D−H (Å)	H···A (Å)	D···A (Å)	D−H···A (deg)
5·MeCN	N−H···S1 (intra)[b]	0.96(2)	2.55(2)	3.1471(19)	120.5(18)
	N−H···S1A (inter)[b]	0.96(2)	2.56(2)	3.3525(18)	139.8(19)
6	N−H···O2A (inter)[c]	0.848(19)	2.088(19)	2.9005(15)	160.4(17)
	N−H···O3A (inter)[c]	0.848(19)	2.309(17)	2.9245(16)	129.7(15)

[a] Data calculated by using the program system PLATON.[5] [b] S1···H···S1A = 80.0(7)°. [c] O2A···H···O3A = 65.3(5)°.

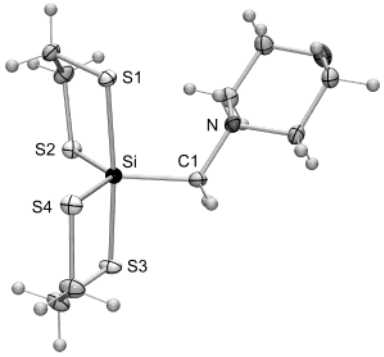

Figure 1. Structure of **5** in the crystal of **5**·MeCN (probability level of displacement ellipsoids 50%).

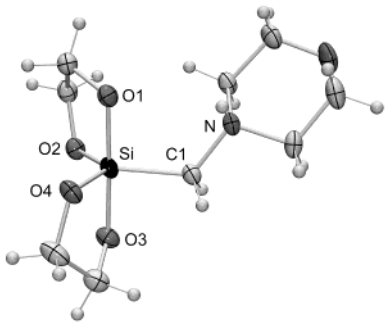

Figure 2. Structure of **6** in the crystal (probability level of displacement ellipsoids 50%).

spanning one axial (S1, S3; O1, O3) and one equatorial site (S2, S4; O2, O4).

As expected from the presence of the potential NH donor functions and the potential sulfur or oxygen acceptor atoms, hydrogen-bonding systems were observed in the crystals of **5**·MeCN and **6** (Table 3, Figures 3 and 4).[5] The zwitterion of **5**·MeCN forms a bifurcate N−H···S1/S1A hydrogen bond, with an intramolecular N−H···S1 and an intermolecular N−H···S1A interaction, leading to the formation of centrosymmetric dimers in the crystal.[6] As a result of this hydrogen bond, the Si−S1 distance is longer than the Si−S3 distance. Compound **6** forms an intermolecular bifurcate N−H ···O2A/O3A hydrogen bond, leading to the formation of infinite chains along [1 0 1]. This interaction results in an elongation of the Si−O3 bond compared to the Si−O1 bond.

Solid-State NMR Studies. Compounds **5**·MeCN and **6** were characterized by solid-state VACP/MAS NMR experiments (^{13}C, ^{29}Si) at 22 °C. The NMR spectra

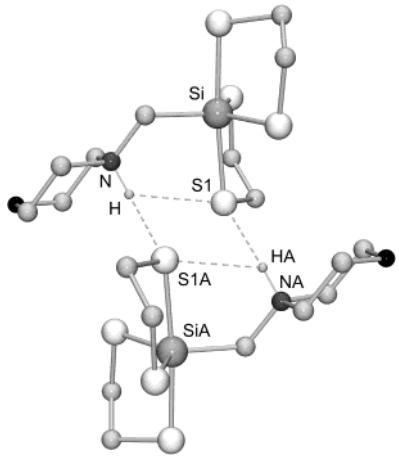

Figure 3. Hydrogen-bonding system in the crystal of **5**·MeCN. The dashed lines indicate bifurcate hydrogen bonds, with an intra- and an intermolecular interaction, leading to the formation of centrosymmetric dimers. The hydrogen atoms (except for the N*H* atoms) are omitted for clarity.

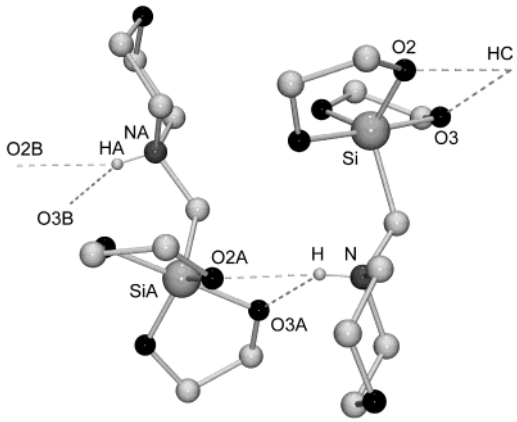

Figure 4. Hydrogen-bonding system in the crystal of **6**. The dashed lines indicate intermolecular bifurcate hydrogen bonds, leading to the formation of infinite chains. The hydrogen atoms (except for the N*H* atoms) are omitted for clarity.

obtained (see Experimental Section) are compatible with the crystal structures of **5**·MeCN and **6**. The isotropic ^{29}Si chemical shifts (**5**·MeCN, $\delta = -64.1$ ppm; **6**, $\delta = -90.0$ ppm) are typical of an SiS_4C and SiO_4C skeleton, respectively, and are similar to those of related zwitterionic $\lambda^5 Si$-silicates with two bidentate ethane-1,2-dithiolato(2−)[2] or ethane-1,2-diolato(2−)[7] ligands.

The isotropic ^{29}Si chemical shift is not the only source of information in high-resolution solid-state NMR spectroscopy. The anisotropy of the ^{29}Si chemical shift is expected to respond very sensitively to structure and bonding. In the case of **5**·MeCN and **6**, a correlation of

(5) The hydrogen-bonding systems were analyzed by using the program system PLATON: Spek, A. L. PLATON; University of Utrecht: Utrecht, The Netherlands, 1998. In this context, see also: Jeffrey, G. A.; Saenger, W. *Hydrogen Bonding in Biological Structures*; Springer-Verlag: Berlin, Germany, 1991; pp 15−24.

(6) The acetonitrile is not involved in the hydrogen-bonding system. Treatment of **5**·MeCN in vacuo at 20 °C over a period of ca. 16 h leads to a complete loss of the acetonitrile.

(7) Tacke, R.; Pülm, M.; Richter, I.; Wagner, B.; Willeke, R. *Z. Anorg. Allg. Chem.* **1999**, *625*, 2169−2177.

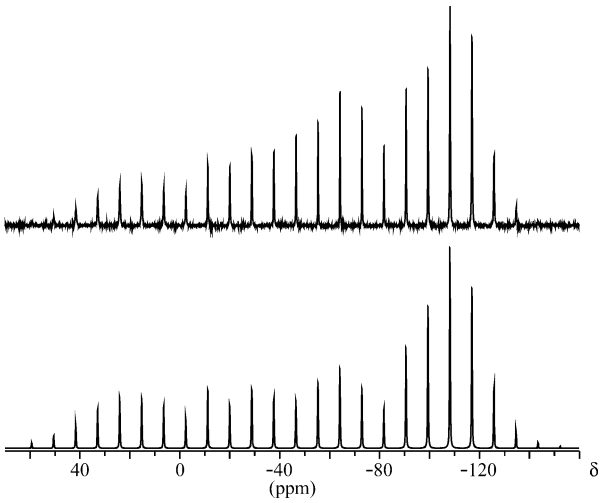

Figure 5. Comparison of the experimental solid-state ^{29}Si VACP/MAS NMR spectrum of **5**·MeCN at a spinning rate of 702 Hz (above) and the simulated spectrum obtained with the program system WIN-MAS[16] (below).

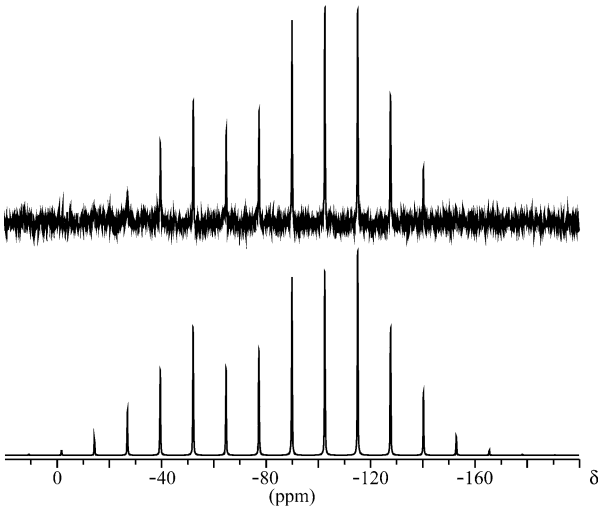

Figure 6. Comparison of the experimental solid-state ^{29}Si VACP/MAS NMR spectrum of **6** at a spinning rate of 1003 Hz (above) and the simulated spectrum obtained with the program system WIN-MAS[16] (below).

the tensor components of the ^{29}Si chemical shift anisotropy with the geometry of the Si-coordination polyhedron (trigonal bipyramid) was anticipated. The quality of the ^{29}Si VACP/MAS NMR spectra of **5**·MeCN (**6**) recorded at a spinning rate of 702 Hz (1003 Hz) (Figures 5 and 6) was good enough to evaluate the tensor components by simulation of the spinning sideband pattern (in this context, see ref 8). The results of the simulations for **5**·MeCN (**6**) are as follows.[9] Isotropic chemical shift: $\delta_{iso} = -64.2$ (-90.0) ppm; chemical shift anisotropy components: $\delta_{11} = -125.7$ (-146.9) ppm, $\delta_{22} = -117.7$ (-103.6) ppm, $\delta_{33} = +50.9$ (-19.4) ppm; anisotropy parameter: $\Delta\delta = \delta_{33} - \delta_{iso} = +115.1$ ($+70.6$) ppm; asymmetry parameter: $\eta = (\delta_{22} - \delta_{11})(\Delta\delta)^{-1} =$ 0.07 (0.61). The small η value for **5**·MeCN indicates an almost axially symmetric shift tensor ($\delta_{22} \approx \delta_{11}$), whereas the η value for **6** indicates a rhombic shift tensor. These results are in good agreement with the computed chemical shift tensors of the Si-coordination polyhedra of **5** and **6** (see Quantum Chemical Calculations). It should be mentioned, however, that the analysis of the anisotropic chemical shift components in the range of axial or nearly axial symmetry, based on the method reported in ref 8b, involves uncertainties. On the other hand, the results of the simulations are in good agreement with the experimentally established spinning sideband patterns of the solid-state ^{29}Si VACP/MAS NMR signals at 702 Hz (1003 Hz) spinning frequency and are consistent with the experimentally established crystal structures of **5**·MeCN and **6**.

Table 4. Compositions of the NLMOs around the Silicon Atoms of 5 and 6[a]

	% X (% C) character	
NLMO	**5** (X = S)	**6** (X = O)
Si−X1 (ax)	74.8	84.8
Si−X2 (eq)	68.4	84.3
Si−X3 (ax)	72.1	85.7
Si−X4 (eq)	68.0	84.3
Si−C1 (eq)	73.8	76.8

[a] BLYP/TZP results obtained for the experimentally established structures. The relative contribution of the substituent's natural atomic orbital (NAO) to a given NLMO is provided as an indication of bond ionicity.

Quantum Chemical Calculations. As currently available DFT methods tend to overestimate bond lengths in the case of heavier p-block elements such as silicon and sulfur,[10] we have used the well-established RI-MP2 method[11] for structure optimizations. The RI-MP2/TZP optimizations of the isolated molecules **5** and **6** converged to similar structures, as found experimentally in the crystal structure analyses of **5**·MeCN and **6**, but with a number of notable differences (Table 2): Due to the neglect of intermolecular hydrogen bonding, the intramolecular N−H···S1 and N−H···O1 hydrogen bond strength is overestimated by the calculations compared to the bifurcate hydrogen-bonding systems in the crystal structures of **5**·MeCN and **6**. This leads to a notably lengthened Si−S1 and Si−O1 bond (Table 2), whereas the computed Si−S3 and Si−O3 distances are only slightly shorter than the respective experimental values. In the presence of an additional intermolecular hydrogen bond (calculations on the centrosymmetric dimer of **5**), a significantly better agreement between the calculated and experimentally established values was found (Table 2). The calculated centrosymmetric dimer of **5** is 54.5 kJ mol^{-1} energetically more favored than two monomers (including the counterpoise correction (CP)[12]).

Due to the obvious structural effects of intermolecular hydrogen bonding, the bonding analysis and NMR chemical shift calculations for **5** and **6** were performed on the experimentally established structures of **5**·MeCN and **6** (i.e., on the monomeric structures cut out of the dimeric or polymeric structures, respectively, in the

(8) (a) Maricq, M. M.; Waugh, J. S. *J. Chem. Phys.* **1979**, *70*, 3300−3316. (b) Herzfeld, J.; Berger, A. E. *J. Chem. Phys.* **1980**, *73*, 6021−6030. (c) Clayden, N. J.; Dobson, C. M.; Lian, L.-Y.; Smith, D. J. *J. Magn. Reson.* **1986**, *69*, 476−487.

(9) The tensor components were denoted in terms of chemical shift anisotropy as computed by using the program system WIN-MAS, reflecting the chemical point of view that a strongly shielded nucleus is characterized by negative chemical shift values.

(10) (a) Kaupp, M. *Chem. Ber.* **1996**, *129*, 535−544. (b) Altmann, J. A.; Handy, N. C.; Ingamells, V. E. *Mol. Phys.* **1997**, *92*, 339−352.

(11) Schrodt, C.; Weigend, F.; Ahlrichs, R. *Z. Anorg. Allg. Chem.* **2002**, *628*, 2478−2482.

(12) Boys, S. F.; Bernardi, F. *Mol. Phys.* **1970**, *19*, 553−566.

Table 5. Major LMO Contributions (ppm) to the Computed (IGLO-UDFT) Absolute Nuclear Shieldings of 5 and 6[a]

	σ_{iso}		σ_{11}		σ_{22}		σ_{33}	
LMO	**5**[b]	**6**[c]	**5**[b]	**6**[c]	**5**[b]	**6**[c]	**5**[b]	**6**[c]
Si K-shell	481.7	481.7	481.7	481.7	481.7	481.7	481.7	481.7
Si L-shell	307.7	328.3	311.0	329.9	307.9	332.8	304.2	322.2
$Bd(Si-X1)_{ax}$	−45.0	−68.7	−74.0	−102.5	−65.2	−107.6	4.1	4.1
$Bd(Si-X2)_{eq}$	−93.4	−53.2	−51.9	−7.2	−30.8	−44.8	−197.6	−107.4
$Bd(Si-X3)_{ax}$	−59.0	−64.3	−98.3	−98.8	−83.1	−98.8	4.5	4.7
$Bd(Si-X4)_{eq}$	−95.2	−49.3	5.7	−7.6	−94.0	−37.5	−197.4	−102.8
$Bd(Si-C1)_{eq}$	−80.6	−78.0	−81.6	−79.0	−15.1	5.9	−145.0	−160.9
$\sum LP(X)_{ax}$	−11.7	3.0	−25.3	−8.9	−29.3	−13.7	9.3	31.5
$\sum LP(X)_{eq}$	0.6	−51.4	−5.3	−0.4	−3.7	−62.2	0.2	−91.8
$\sum$[d]	405.1	448.1	462.0	507.2	468.4	455.8	264.0	381.3
total[e]	397.2	435.4	465.6	503.2	457.4	432.7	268.7	370.2

[a] Only the most important contributions from localized molecular orbitals are provided. Further small contributions come from, for example, C−C bonding LMOs. [b] X = S. [c] X = O. [d] Sum of displayed contributions. [e] Total computed shielding values.

crystal). NBO analyses provide well-localized Lewis structures (with only 1.1% non-Lewis NBO contributions to the one-particle density matrix for both compounds), indicating five fairly ionic bonds to silicon. The compositions of the Si−X (X = S, O) and Si−C natural localized molecular orbitals (NLMOs), based on these Lewis structures, are shown in Table 4. For compound **6**, all four Si−O bonding NLMOs are nearly identical and more strongly polarized than the Si−C1 NLMO (as expected from the different electronegativities of oxygen and carbon), whereas in the case of **5** the axial Si−S1 and Si−S3 bonding NLMOs are somewhat more polarized toward sulfur than the equatorial Si−S2 and Si−S4 NLMOs. Notably, the Si−C1 NLMO is even slightly more polarized than the equatorial Si−S2 and Si−S4 NLMOs. This may be due to the rather electronegative morpholinium nitrogen substituent on the C1 atom. The differences between the axial and equatorial Si−S bonding NLMOs are clearly less pronounced than one might expect from a simplified bonding picture with one axial three-center bond and three equatorial two-center bonds. This is consistent with the results of a more elaborate analysis of PF_5.[13] The overall bonding situation in **5** and **6** is consistent with those of other pentacoordinate compounds of p-block main group elements in exhibiting very polar bonds and a significant positive charge on the central atom (the calculated natural charge on the silicon atom amounts to +1.02 (**5**) and +2.16 (**6**)). This positive charge is a major prerequisite of hypercoordination.[14] Obviously, even the combination of four sulfur atoms and one carbon atom does not prevent the required high bond ionicity when attached to silicon as the central atom.

The BLYP-GIAO calculations of the ^{29}Si chemical shift tensors of **5** (**6**), computed using the experimentally established structures of **5**·MeCN and **6**, gave the following results: δ_{iso} = −49.9 (−90.3) ppm, δ_{11} = −117.7 (−156.9) ppm, δ_{22} = −104.9 (−83.6) ppm, δ_{33} = +72.9 (−30.3) ppm. As expected (for a recent review, see ref 15), these UDFT calculations with gradient-corrected density functionals agree with the experimental shift tensor contributions within ca. 10−20 ppm. The calculations reproduce the nearly axial (**5**) and rhombic (**6**) tensors. In particular, they provide the orientation of the most deshielded δ_{33} components, which point almost exactly along the axial Si−S and Si−O bond vectors. The slight asymmetry of the tensors for **5** (η = 0.10) and the strong asymmetry of the tensors for **6** (η = 1.22) are also in reasonable agreement with the experimental data (**5**, η = 0.07; **6**, η = 0.61). Note that shielding tensor components from a calculation on the hydrogen-bonded dimer of **5** deviate only by ca. 2 ppm from the calculation on the monomer.

Subsequent BLYP-IGLO calculations allowed a breakdown of the shielding tensor components into contributions from occupied localized molecular orbitals (LMOs). The overall shift tensor results agree well with the GIAO calculations. The most important LMO contributions to the absolute ^{29}Si nuclear shieldings are summarized in Table 5. The analyses clearly show that for both compounds the large δ_{33} (low σ_{33}) tensor component is due to dominant contributions from the equatorial bonding LMOs, in particular the Si−S2 (Si−O2) and Si−S4 (Si−O4) bonds, but also the Si−C1 bond. However, in the case of **6** the contributions from the lone pairs localized at the oxygen atoms are even larger than those localized at the sulfur atoms of **5**. Obviously, the external magnetic field induces the largest ring currents in the plane of the three equatorial ligand atoms. This might seem surprising at first glance, as one would expect smaller energy denominators in the paramagnetic shielding expressions involving the axial bonds, and thus large shift tensor components in the equatorial plane. However, closer inspection reveals that the lower ionicity of the equatorial bonds (see the NLMO composition in Table 4) produces larger orbital Zeeman and, in particular, paramagnetic spin−orbit matrix elements, and thereby larger paramagnetic contributions in the axial direction.

Conclusions

Apparently, an SiS$_4$C skeleton is not a real curiosity in the chemistry of higher-coordinate silicon but may be stabilized more generally than previously thought. The detailed bonding analysis has indicated that all five bonds in the SiS$_4$C framework of **5** are significantly and almost equally polarized toward the ligand atoms. This is inconsistent with a bonding picture with an axial three-center bond but rather emphasizes the necessity of polar bonds to stabilize such a hypercoordinate silicon center.

(13) Häser, M. *J. Am. Chem. Soc.* **1996**, *118*, 7311−7325.
(14) See, e.g.: Reed, A. E.; Schleyer, P. v. R. *J. Am. Chem. Soc.* **1990**, *112*, 1434−1445, and references therein.
(15) Review dealing with DFT calculations of NMR chemical shifts: Bühl, M.; Kaupp, M.; Malkina, O. L.; Malkin, V. G. *J. Comput. Chem.* **1999**, *20*, 91−105.

The most deshielded component of the ^{29}Si chemical shift tensors in both **5** and **6** has been shown to point along the axial bonds. While this seems to be a characteristic feature of the approximately trigonal-bipyramidal Si-coordination polyhedra, the tensor is almost axially symmetric for **5** but significantly rhombic for **6**. The latter point appears to reflect the almost identical ionicity of the equatorial Si−S and Si−C bonds in **5** compared to the significantly larger ionicity of the Si−O bonds in **6**.

Experimental Section

General Procedures. All syntheses were carried out under dry argon. The organic solvents used were dried and purified according to standard procedures and stored under nitrogen. Melting points were determined with a Büchi melting point B-540 apparatus using samples in sealed capillaries. The ^{1}H, ^{13}C, and ^{29}Si solution NMR spectra were recorded at 22 °C on a Bruker DRX-300 NMR spectrometer (^{1}H, 300.1 MHz; ^{13}C, 75.5 MHz; ^{29}Si, 59.6 MHz). C_6D_6 served as the solvent. Chemical shifts (ppm) were determined relative to internal C_6D_5H (^{1}H, δ 7.28), internal C_6D_6 (^{13}C, δ 128.0), or external TMS (^{29}Si, δ 0). Solid-state ^{13}C and ^{29}Si VACP/MAS NMR spectra were recorded at 22 °C on a Bruker DSX-400 NMR spectrometer with bottom layer rotors of ZrO_2 (diameter 7 mm) containing ca. 300 mg of sample (^{13}C, 100.6 MHz; ^{29}Si, 79.5 MHz; external standard, TMS (^{13}C and ^{29}Si, δ 0); spinning rate, 5 kHz; contact time, 1 ms (^{13}C) or 5 ms (^{29}Si); 90° ^{1}H transmitter pulse length, 3.6 μs; repetition time, 4 s). The chemical shift anisotropy of the ^{29}Si resonances of **5**·MeCN (**6**) was calculated by simulation of the ^{29}Si VACP/MAS NMR spectra recorded at a spinning rate of 702 Hz (1003 Hz) using the program system WIN-MAS.[16]

Preparation of Bis[ethane-1,2-dithiolato(2−)](morpholiniomethyl)silicate−Acetonitrile (5·MeCN). Compound **8** (109 mg, 830 μmol) was added dropwise within 2 min at 20 °C to a stirred solution of ethane-1,2-dithiol (156 mg, 1.66 mmol) in acetonitrile (7 mL) (slow evolution of hydrogen). The mixture was kept undisturbed for 5 h at 20 °C (end of hydrogen evolution) and then for a further 48 h at −26 °C (formation of crystals). The resulting precipitate was isolated by filtration, washed with cold (−26 °C) acetonitrile (3 × 2 mL), and dried in an argon gas stream to give **5**·MeCN in 86% yield as a colorless crystalline solid (253 mg, 713 μmol); mp 93 °C (dec). ^{13}C VACP/MAS NMR (13117 transients): δ 6.4 (CH_3CN), 33.3 (SCH_2C), 35.0 (2 C) (SCH_2C), 36.2 (SCH_2C), 53.7, 56.7, and 58.1 (3 C, NCH_2C and $SiCH_2N$), 63.8 (OCH_2C), 64.4 (OCH_2C), 117.8 (CH_3CN). ^{29}Si VACP/MAS NMR (155 transients): δ −64.1. Anal. Calcd for $C_{11}H_{22}N_2OS_4Si$ (354.7): C 37.25, H 6.25, N 7.90, S 36.17. Found: C 37.2, H 6.3, N 7.8, S 36.0.

Preparation of Bis[ethane-1,2-diolato(2−)](morpholiniomethyl)silicate (6). Compound **7** (357 mg, 1.61 mmol) was added dropwise within 2 min at 20 °C to a stirred solution of ethane-1,2-diol (200 mg, 3.22 mmol) in acetonitrile (10 mL), and the reaction mixture was then kept undisturbed at 20 °C for 24 h. The resulting precipitate was isolated by filtration and recrystallized from dichloromethane/diethyl ether (1:2 (v:v)). The crystalline product was washed with diethyl ether (10 mL) and dried in vacuo to give **6** in 80% yield as a colorless crystalline solid (319 mg, 1.28 mmol); mp 93 °C. ^{13}C VACP/MAS NMR (2096 transients): δ 48.8, 51.3, and 56.5 (3 C, NCH_2C and $SiCH_2N$), 60.2 (2 C) ($O(CH_2)_2O$), 61.1 (2 C) ($O(CH_2)_2O$), 64.3 (OCH_2C), 64.5 (OCH_2C). ^{29}Si VACP/MAS NMR (380 transients): δ −90.0. Anal. Calcd for $C_9H_{19}NO_5Si$ (249.3): C 43.35, H 7.68, N 5.62. Found: C 42.8, H 7.6, N 5.7.

Preparation of Trimethoxy(morpholinomethyl)silane (7). This compound was synthesized according to ref 17.

Preparation of (Morpholinomethyl)silane (8). A solution of **7** (5.41 g, 24.4 mmol) in diethyl ether (20 mL) was added at 0 °C within 1 h to a vigorously stirred suspension of lithium aluminum hydride (970 mg, 25.6 mmol) in diethyl ether (20 mL). The resulting mixture was stirred at 20 °C for 18 h and then under reflux for a further 2 h. After the suspension was filtered, the solvent of the filtrate was removed under reduced pressure, and the residue was distilled in vacuo to give **8** in 61% yield as a colorless liquid (1.97 g, 15.0 mmol); bp 35 °C/15 mbar. ^{1}H NMR: δ 1.92 (q, $^{3}J_{HH}$ = 3.6 Hz, $^{2}J_{SiH}$ = 5.5 Hz, 2 H, $SiCH_2N$), 2.21−2.29 (m, 4 H, NCH_2C), 3.61−3.67 (m, 4 H, OCH_2C), 3.71 (t, $^{3}J_{HH}$ = 3.6 Hz, $^{1}J_{SiH}$ = 196.5 Hz, 3 H, Si*H*). ^{13}C{^{1}H} NMR: δ 41.2 ($SiCH_2N$), 56.8 (NCH_2C), 67.1 (OCH_2C). ^{29}Si NMR: δ −66.7 (qt, $^{1}J_{SiH}$ = 196.5 Hz, $^{2}J_{SiH}$ = 5.5 Hz). Anal. Calcd for $C_5H_{13}NOSi$ (131.3): C 45.76, H 9.98, N 10.67. Found: C 45.6, H 10.2, N 10.7.

Single-Crystal X-ray Diffraction Studies. Suitable single crystals of **5**·MeCN and **6** were obtained directly from the respective reaction mixtures. The crystals were mounted in inert oil (perfluoroalkyl ether, ABCR) on a glass fiber and then transferred to the cold nitrogen gas stream of the diffractometer (Stoe IPDS diffractometer, graphite-monochromated Mo Kα radiation (λ = 0.71073 Å)). The structures were solved by direct methods.[18] The non-hydrogen atoms were refined anisotropically.[19] A riding model was employed in the refinement of the C*H* hydrogen atoms. The N*H* hydrogen atoms were localized in difference Fourier syntheses and refined freely.

Computational Studies. The structures of **5** and **6** were optimized at the RI-MP2 level[20] using a TZP basis set[21] and a TZVP auxiliary basis for the fit of the charge density.[22] The calculations were performed starting from the structures of the zwitterions in the crystals of **5**·MeCN and **6** and using the TURBOMOLE program system.[23] The optimized structures were characterized as minima on the potential energy surfaces by harmonic vibrational frequency analysis.[24]

The ^{29}Si NMR chemical shift calculations implied the experimental structural parameters of **5** and **6** and were initially carried out at the uncoupled density-functional theory (UDFT) level[25] using the program system GAUSSIAN 98,[26]

(16) Program system WIN-MAS (version 951208); Bruker-Franzen Analytik GmbH: Bremen, Germany, 1995.

(17) Sperlich, J.; Becht, J.; Mühleisen, M.; Wagner, S. A.; Mattern, G.; Tacke, R. *Z. Naturforsch.* **1993**, *48b*, 1693−1706.
(18) Sheldrick, G. M. SHELXS-97; University of Göttingen: Göttingen, Germany, 1997. Sheldrick, G. M. *Acta Crystallogr., Sect. A* **1990**, *46*, 467−473.
(19) Sheldrick, G. M. SHELXL-97; University of Göttingen: Göttingen, Germany, 1997.
(20) (a) Weigend, F.; Häser, M. *Theor. Chem. Acc.* **1997**, *97*, 331−340. (b) Weigend, F.; Häser, M.; Patzelt, H.; Ahlrichs, R. *Chem. Phys. Lett.* **1998**, *294*, 143−152.
(21) Schäfer, A.; Horn, H.; Ahlrichs, R. *J. Chem. Phys.* **1992**, *97*, 2571−2577.
(22) Schäfer, A.; Huber, C.; Ahlrichs, R. *J. Chem. Phys.* **1994**, *100*, 5829−5835.
(23) Program system TURBOMOLE: Ahlrichs, R.; Bär, M.; Häser, M.; Horn, H.; Kölmel, C. *Chem. Phys. Lett.* **1989**, *162*, 165−169.
(24) The structures of **5**·MeCN and **6** were calculated starting from the respective geometry obtained by the crystal structure analyses of **5**·MeCN and **6**. However, a more stable minimum for **6** (data not given) was found by calculation, featuring the same envelope conformation of the two five-membered rings as observed (calculated) for **5**·MeCN (**5**).
(25) In this context, see: Malkin, V. G.; Malkina, O. L.; Casida, M. E.; Salahub, D. R. *J. Am. Chem. Soc.* **1994**, *116*, 5898−5908.
(26) Frisch, M. J.; Trucks, G. W.; Schlegel, H. B.; Scuseria, G. E.; Robb, M. A.; Cheeseman, J. R.; Zakrzewski, V. G.; Montgomery, J. A., Jr.; Stratmann, R. E.; Burant, J. C.; Dapprich, S.; Millam, J. M.; Daniels, A. D.; Kudin, K. N.; Strain, M. C.; Farkas, O.; Tomasi, J.; Barone, V.; Cossi, M.; Cammi, R.; Mennucci, B.; Pomelli, C.; Adamo, C.; Clifford, S.; Ochterski, J.; Petersson, G. A.; Ayala, P. Y.; Cui, Q.; Morokuma, K.; Malick, D. K.; Rabuck, A. D.; Raghavachari, K.; Foresman, J. B.; Cioslowski, J.; Ortiz, J. V.; Baboul, A. G.; Stefanov, B. B.; Liu, G.; Liashenko, A.; Piskorz, P.; Komaromi, I.; Gomperts, R.; Martin, R. L.; Fox, D. J.; Keith, T.; Al-Laham, M. A.; Peng, C. Y.;

gauge-including atomic orbitals (GIAOs),[27] and the BLYP functional.[28] For these calculations, the extended basis set B-II (sometimes referred to as IGLO-II basis) of Kutzelnigg et al.[29] was used for the silicon atoms and for the ligand atoms directly bonded to silicon. More contracted DZVP basis sets[30] were used for all the other atoms. Computed absolute shieldings (σ) were converted to relative shifts (δ) using the shielding of TMS (327.3 ppm), computed at the same theoretical level (BLYP-GIAO). For subsequent calculations, the MO information from the BLYP calculation was transferred via an interface program to the in-house property program system MAG-ReSpect.[31] This was subsequently used to carry out further UDFT calculations using individual gauges for localized orbitals (IGLO).[29] This allowed detailed analyses of the shift tensors in terms of localized molecular orbitals (LMOs). For the natural bond orbital (NBO) analyses, the built-in NBO-3.0 routines of the GAUSSIAN 98 program system were used.[26]

Acknowledgment. This work was supported by the Deutsche Forschungsgemeinschaft (Graduiertenkolleg "Electron Density: Theory and Experiment") and the Fonds der Chemischen Industrie.

Supporting Information Available: Tables of atomic coordinates and equivalent isotropic displacement parameters, anisotropic displacement parameters, experimental details of the X-ray diffraction study, and bond lengths and angles for **5**·MeCN and **6**; figures showing the calculated structures (geometry optimizations) of **5** (monomer and dimer) and **6**. This material is available free of charge via the Internet at http://pubs.acs.org. In addition, crystallographic data (excluding structure factors) for the structures reported in this paper have been deposited with the Cambridge Crystallographic Data Centre as supplementary publication nos. CCDC-205722 (**5**·MeCN) and CCDC-205723 (**6**). Copies of the data can be obtained free of charge on application to CCDC, 12 Union Road, Cambridge CB2 1EZ, UK (fax: (+44) 1223/336033; e-mail: deposit@ccdc.cam.ac.uk).

OM030301S

Nanayakkara, A.; Gonzalez, C.; Challacombe, M.; Gill, P. M. W.; Johnson, B. G.; Chen, W.; Wong, M. W.; Andres, J. L.; Head-Gordon, M.; Replogle, E. S.; Pople, J. A. GAUSSIAN 98, revision A.7; Gaussian, Inc.: Pittsburgh, PA, 1998.

(27) See, e.g.: (a) Ditchfield, R. *Mol. Phys.* **1974**, *27*, 789−807. (b) Wolinski, K.; Hinton, J. F.; Pulay, P. *J. Am. Chem. Soc.* **1990**, *112*, 8251−8260.

(28) (a) Becke, A. D. *Phys. Rev. A* **1988**, *38*, 3098−3100. (b) Lee, C.; Yang, W.; Parr, R. G. *Phys. Rev. B* **1988**, *37*, 785−789. (c) Miehlich, B.; Savin, A.; Stoll, H.; Preuss, H. *Chem. Phys. Lett.* **1989**, *157*, 200−206.

(29) Kutzelnigg, W.; Fleischer, U.; Schindler, M. In *NMR Basic Principles and Progress*; Diehl, P., Fluck, E., Günther, H., Kosfeld, R., Seelig, J., Eds.; Springer-Verlag: Berlin, Heidelberg, Germany, 1990; Vol. 23, pp 165−262.

(30) Godbout, N.; Salahub, D. R.; Andzelm, J.; Wimmer, E. *Can. J. Chem.* **1992**, *70*, 560−571.

(31) Malkin, V. G.; Malkina, O. L.; Reviakine, R.; Schimmelpfennig, B.; Arbuznikov, A.; Kaupp, M. MAG-ReSpect, version 1.0; University of Würzburg: Würzburg, Germany, and Slovak Academy of Sciences: Bratislava, Slovakia, 2002.